A Nondimensional Evaluation of Tracer Sensitivity to Density Effects

by Marc Jalbert[a], Jacob H. Dane[a], Linda M. Abriola[b], and Kurt D. Pennell[c]

Abstract

The purpose of this paper is to assess the importance of the density difference between a tracer solution and ground water on the determination of aquifer properties by inversion of tracer signals. To estimate the effect of this density difference, we developed a nondimensional, approximate solution to a Boundary Value Problem (BVP) based on a partial differential equation first presented by Bear and Dagan (1964). The BVP models the displacement of water by another aqueous solution with a different density in a rectangular, vertical cross section of a homogeneous porous medium. A rectangular sandbox analog model was used to verify the validity of the nondimensional solution for the case of a moving interface during the displacement of water by a heavier-than-water aqueous solution. A constant flow rate was maintained by applying constant heads at a fully penetrating vertical inflow and outflow chamber. The theory, which can be applied as a prediction tool for laboratory experiments, permits us to explore the implications of using denser-than-water tracers for determining aquifer hydraulic conductivity and dispersion coefficient values. According to our assessments, density effects should not be ignored, as small density differences can lead to serious uncertainties in permeability and dispersivity determinations.

Introduction

The flow of two aqueous solutions having different densities has been investigated in numerous studies associated with the movement of the salt water/fresh water interface in coastal aquifers. Besides these studies, another branch of ground water modeling makes extensive use of conservative tracers to determine properties of aquifers such as hydraulic conductivity and dispersivity. The influence of the specific gravity difference between ground water and a tracer solution on the transport of the tracer is, however, generally neglected. One possible reason for this omission is that in case of a density difference between ground water and tracer solution, a correct interpretation of the collected data requires a sophisticated computer program capable of inversely simulating the convective-dispersive, density-affected transport of the tracer. The purpose of this paper is to estimate the importance of density differences on a conservative tracer experiment, by providing a simple nondimensional solution to a Boundary Value Problem (BVP) based on a partial differential equation developed in the early research on sea water intrusion (Bear and Dagan 1964). The BVP models the displacement of the ground water by another miscible fluid phase with a different density in a rectangular, vertical cross section of a homogeneous porous medium. The proposed solution, even though it is approximate, shows agreement with experimental data collected in an intermediate-scale sandbox analog model in which water was displaced by a sodium-bromide solution. Flow and transport were maintained between two constant head, fully penetrating vertical inflow and outflow chambers. Consequently, the solution can be applied to laboratory research involving the flow of two aqueous phases having different densities. The nondimensional solution

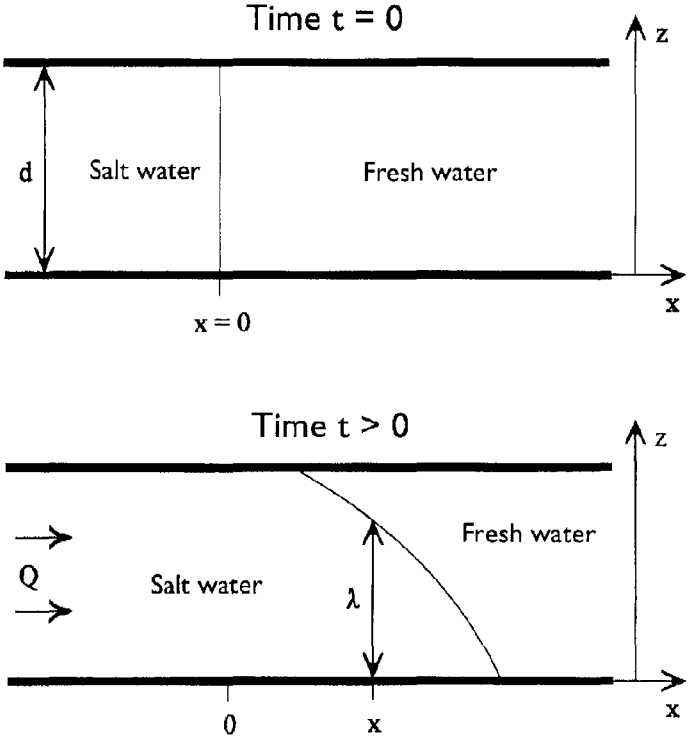

Figure 1. Depiction in vertical cross section of a moving salt water/fresh water sharp interface, at times t = 0 and t > 0.

[a]Department of Agronomy and Soils, Auburn University, AL 36849-5412; jdane@acesag.auburn.edu

[b]Department of Civil and Environmental Engineering, University of Michigan, Ann Arbor, Michigan

[c]School of Civil and Environmental Engineering, Georgia Institute of Technology, Atlanta, Georgia

Received April 1999, accepted October 1999.

is used to estimate the sensitivity of hydraulic conductivity and dispersion determinations to the density difference between the tracer solution and the ambient water. We found that even small density differences can result in substantial errors in the values of aquifer properties obtained by inversion of tracer signals.

Theory

In an infinitely long, horizontal aquifer of thickness d (L), having a saturated hydraulic conductivity K (LT^{-1}) and a porosity n, a vertical interface between two liquids with specific gravities γ_f (fresh water) and γ_s (salt water) is allowed to exist at position x = 0 (L), at time t = 0 (T). For t > 0, a lateral inflow per unit width, Q (L^2T^{-1}), at one end of the aquifer and an equivalent outflow at the other end of the aquifer causes the interface to move and change its slope due to density effects (Figure 1). Considering the Dupuit assumption of horizontal flow and no mixing between the two fluids, the height of the salt water above the bottom of the aquifer, $\lambda(x,t)$, is given by the solution of the Boundary Value Problem (BVP) consisting of the governing partial differential equation (Bear and Dagan 1964; Bear 1972) modified to account for the direction of Q:

$$n\frac{\partial\lambda}{\partial t} + \frac{\partial}{\partial x}\left[\frac{Q\lambda}{d} + K'\frac{\lambda(\lambda - d)}{d}\frac{\partial\lambda}{\partial x}\right] = 0 \qquad (1)$$

subjected to the boundary conditions

$$\lambda(x,0) = d \qquad \text{for } x < 0 \qquad (2a)$$

$$\lambda(x,0) = 0 \qquad \text{for } x > 0 \qquad (2b)$$

$$\lambda(-\infty,t) = d \qquad (2c)$$

with $K' = K\cdot(\gamma_s - \gamma_f)/\gamma_f$ being taken positive for the remainder of this study.

Equation 1, subject to Equation 2, can be simplified to the new nondimensional BVP

$$\frac{\partial\Lambda}{\partial T} + \frac{\partial}{\partial X}\left[\Lambda + \Lambda(\Lambda - 1)\frac{\partial\Lambda}{\partial X}\right] = 0 \qquad (3)$$

$$\Lambda(X,0) = 1 \qquad \text{for } X < 0 \qquad (4a)$$

$$\Lambda(X,0) = 0 \qquad \text{for } X > 0 \qquad (4b)$$

$$\Lambda(-\infty,T) = 1 \qquad (4c)$$

where the nondimensional variables Λ, X, T, satisfy

$$\Lambda(X,T) = \frac{\lambda(x,t)}{d} \qquad (5a)$$

$$X = \frac{Q}{d^2K'}x \qquad (5b)$$

$$T = \frac{Q^2}{d^3K'n}t \qquad (5c)$$

If the front is approximated by a straight line (satisfying $\Lambda[X,T] = a[T]\cdot X + b[T]$) at some time, then (disregarding the singularities at $\Lambda = 0$ and $\Lambda = 1$) the second term of the governing Equation 3 is also a linear function of X. Hence, the front will remain a straight line when time progresses. Having a vertical, linear front as the initial condition, the idea is to consider a front that remains linear as time progresses, as an approximate solution of the BVP consisting of Equations 3 and 4. The solution is only approximate because we (1) use the Dupuit assumption of horizontal flow; (2) assume a sharp interface, thus ignoring any diffusion/dispersion of the tracer; (3) use the assumption of a linear front; and (4) disregard the singularities at $\Lambda = 0$ and $\Lambda = 1$. However, because we were interested only in estimating density effects and not in obtaining the exact solution of the nonlinear Equation 1, subjected to Equation 2, we decided to use the linear approximation. This formulation can be easily manipulated and is supported by the experimental results presented in the section Materials and Methods. Given the hypothesis of a linear front, we may consider the situation presented in Figure 2. At some nondimensional time T, the linear front satisfies

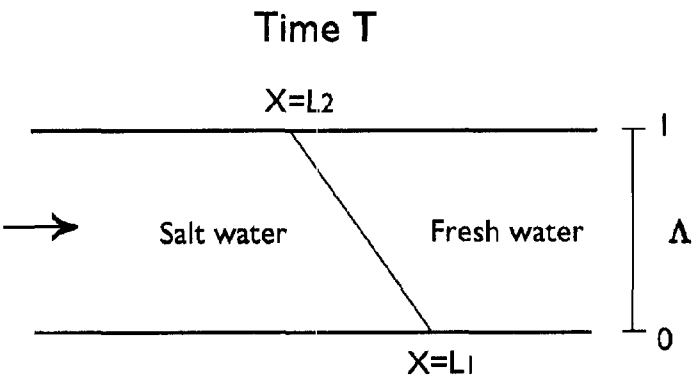

Figure 2. Configuration of a linear approximation of the salt water/fresh water front at nondimensional time T.

$$\begin{cases} X = L_1, & \Lambda = 0 \\ X = L_2, & \Lambda = 1 \end{cases} \qquad (6)$$

The equation for the front is, therefore,

$$\Lambda = \frac{L_1 - X}{L_1 - L_2} \qquad (7)$$

and the formula giving the slope S of the front at time T is

$$S = \frac{\partial\Lambda}{\partial X} = \frac{-1}{L_1 - L_2} \qquad (8)$$

The slope at time T+dT satisfies the expression

$$S(T + dT) = \frac{\partial}{\partial X}[\Lambda(T + dT)] = \frac{\partial}{\partial X}\left[\Lambda(T) + dT\frac{\partial\Lambda(T)}{\partial T}\right] = \frac{\partial\Lambda}{\partial X} + dT\frac{\partial^2\Lambda}{\partial X\partial T} \qquad (9)$$

Substituting Equation 7 into Equation 3 and differentiating with respect to X gives

$$\frac{\partial^2\Lambda}{\partial X\partial T} = \frac{2}{(L_1 - L_2)^3} = -2\cdot S^3 \qquad (10)$$

Equation 9 can then be reformulated as

$$S(T + dT) = S(T) - 2dT[S(T)]^3 \qquad (11)$$

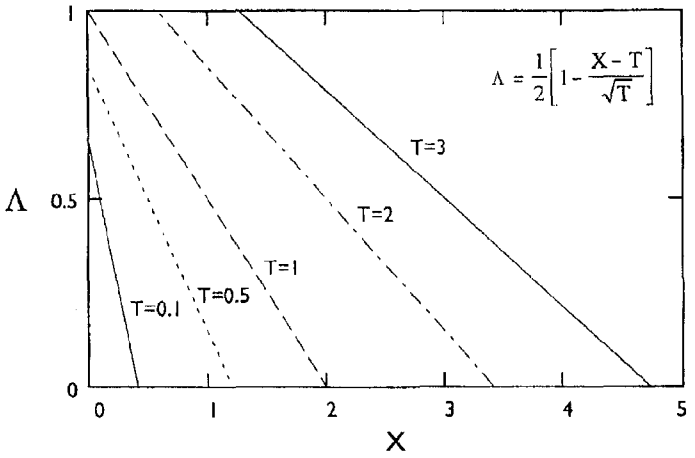

Figure 3. Evolution of the theoretical front as a function of the nondimensional variables (X,Λ,T).

which, upon separation of the variables, yields

$$\frac{dS}{S^3} = -2dT \tag{12}$$

Considering that the inverse of the slope attains a zero value for T = 0, and that in our case of salt water displacing fresh water the derivative of Λ with respect to X is negative, we obtain the evolution of the nondimensional slope of the front with time:

$$S = \frac{\partial \Lambda}{\partial X} = \frac{-1}{2\sqrt{T}} \tag{13}$$

This equation is consistent with the fact that a singularity occurs in Equation 3 for t = 0, where the derivative of γ with respect to x is not defined because of the presence of the vertical front. Applying the mass balance principle gives us the nondimensional, approximate equation, describing the movement of the front:

$$\Lambda(X,T) = 1 \qquad \text{for } X < T - \sqrt{T} \tag{14a}$$

$$\Lambda(X,T) = \frac{1}{2}\left(1 - \frac{X-T}{\sqrt{T}}\right) \qquad \text{for } T - \sqrt{T} < X < T + \sqrt{T} \tag{14b}$$

$$\Lambda(X,T) = 0 \qquad \text{for } X > T + \sqrt{T} \tag{14c}$$

The approximate solution Equation 14 satisfies Equation 3 on each of the domains it is defined for. However, agreement with Equation 3 cannot be reached at the positions $X = T - \sqrt{T}$ and $X = T + \sqrt{T}$, where the approximate solution presents singularities for the slope of the front. A plot of Equation 14 (Figure 3) shows that the absolute value of the slope of the advancing front gradually decreases as time increases (Equation 13). For the nondimensional times T < 1, the mass balance principle is not obeyed in the domain X > 0, because the domain used for the derivation of Equation 14 also includes X < 0. Nevertheless, as we will see later, this inconsistency has little influence on the general flow behavior.

Materials and Methods

In order to verify the validity of Equation 14, an intermediate-scale flow container (internal dimensions: 1.67 m long by 1.0 m high by 5 cm thick, Figure 9) was used to demonstrate the movement of an initially vertical tracer front as it displaced deionized water in a fully saturated porous medium. The flow container, of which a full description can be found in Oostrom et al. (1999), contained a clay layer such that d = 62 cm. No flow was allowed below the clay layer. Above the clay layer, the porous medium consisted of a coarse sand (Table 1) surrounding one lens of a very fine sand (Figure 9, Table 1) and two lenses of a fine sand (Figure 9, Table 1). The average porosity of the coarse sand, as measured with a dual-energy gamma radiation system (Oostrom et al. 1999) was 0.35 (standard deviation = 0.013). The three embedded lenses served little purpose for the research reported in this paper, as they were emplaced to investigate their effect on the infiltration and redistribution of a dense nonaqueous phase liquid in a subsequent experiment. However, these lenses demonstrate the behavior of the front in the presence of heterogeneities. The two end chambers of the flow container allowed for horizontal flow by imposing a head difference along the longitudinal direction. At time t = 0, the deionized water in the inflow chamber was quickly displaced by a 5 g/L NaBr solution dyed with fluorescein ($\Delta\gamma/\gamma_f = 0.0052$), while the fluid level in the chamber was kept constant. The flow rate per unit width (Q) was 2.9×10^{-2} cm^{2}s^{-1}. The successive positions of the front between the deionized water and the salt water were recorded by photography using ultraviolet light.

Supplementary information, in the form of breakthrough curves, was obtained by extracting solution samples as a function of time at a number of ports mounted in the back of the flow container (Figure 9). The samples were analyzed with a bromide specific electrode. The resulting breakthrough curves were analyzed with the program CXTFIT2 (Toride et al. 1995). In this program, developed for one-dimensional problems, pore water velocities (ω) are obtained by dividing the fitted time of the occurrence of the front (breakthrough time) by the longitudinal distance between the injection and observation location. In order to use the obtained values of ω for validation of Equation 14, we need to derive from Equation 14 the time of occurrence of the front ($T = T_O$) at a certain position (X,Z), with Z = z/d, and subsequently divide X by the nondimensional time T_O. We then obtain the nondimensional, apparent velocity field Ω consistent with the hypothesis that lead to Equation 14 and with the one-dimensional CXTFIT2 definition of velocity. Inverting Equation 14 to obtain T as a function of X and Z gives a polynomial of order 2 and, therefore, two solutions. One of these solutions is, however, not applicable to our case and the expression we consider is

$$T_O = \left(-Z + \frac{1}{2} - \frac{1}{2}\sqrt{4Z^2 - 4Z + 1 + 4X}\right)^2 \tag{15}$$

It should be noted that Equation 15 is useful for predicting breakthrough times in case of a step input of a conservative tracer solution with a density that differs from the ambient water. For Ω $= X/T_O$, we obtain Ω, the apparent dimensionless velocity given by one-dimensional inversion, as a function of X and Z:

$$\Omega = \frac{X}{\left(-Z + \frac{1}{2} - \frac{1}{2}\sqrt{4Z^2 - 4Z + 1 + 4X}\right)^2} \tag{16}$$

Table 1
Porous Media Properties

	Porous Medium		
	Sand F4.0	Sand F2.8	Sand F75
Texture	Coarse	Fine	Very Fine
Particle size (% total mass)			
<106 μm	0.07	0.44	2.70
106–250 μm	0.86	14.35	47.53
250–500 μm	7.88	42.52	49.69
500–840 μm	90.47	42.55	0.02
>840 μm	0.07	0.44	0
Porosity	0.35	0.36	0.41
Standard deviation	0.012	0.014	0.019
Bulk density (kg m^{-3})	1696	1566	1556

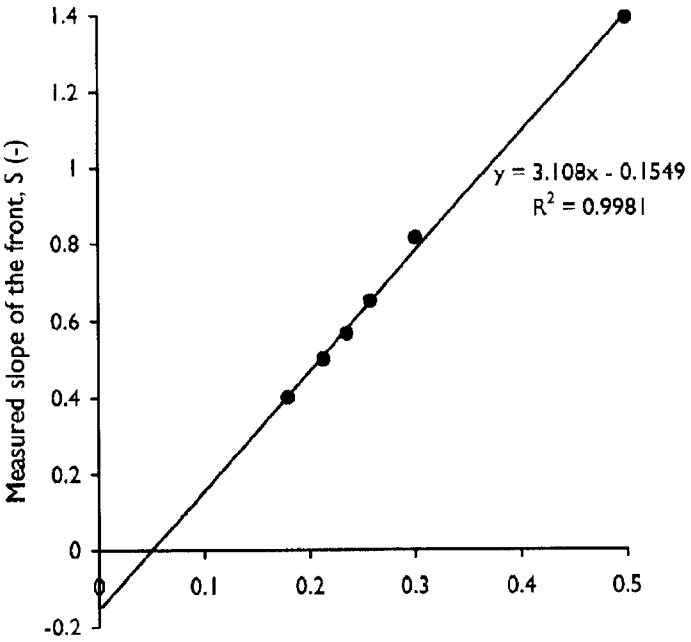

Figure 4. Average slope of the front as a function of the inverse of the square root of time (Equation 9).

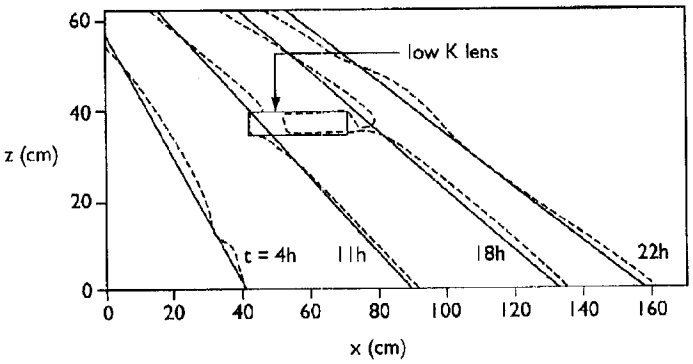

Figure 5. Evolution of the theoretical front as a function of the dimensional variables (x,z,t) for the intermediate-scale experiment and comparison with actual experimental fronts.

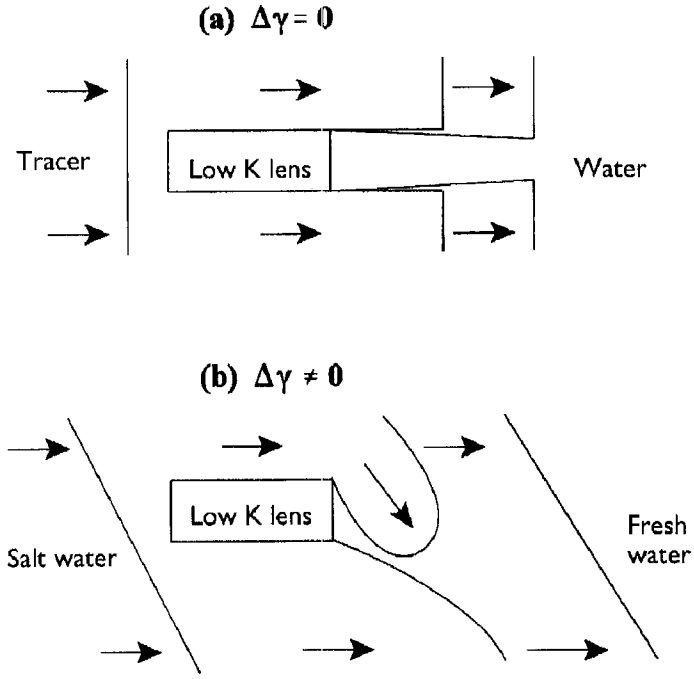

Figure 6. Behavior of the front at the proximity of a low permeability lens: cases of (a) zero density difference and (b) nonzero density difference between tracer solution and water.

fluids only, is not consistent with the boundary condition

$$\lambda(-\infty,t) = d \tag{2c}$$

used for developing Equation 14, but instead imposes the boundary condition

$$\lambda(x,t) = d \qquad \text{for } x < 0 \tag{17}$$

on the flow of the sodium-bromide solution. Consequently, our experimental results show a weak influence of the boundary condition on the general behavior of the front, and support the approximations made during the development of our model. For instance, the assumption of a linear front is generally valid, and other similar experiments not presented here confirm this behavior. The best agreement with the linear approximation is generally found at intermediate and long times, when the front is far enough from the influence of the inflow chamber, i.e., when the boundary condition Equation 2c gains validity. This result is also logical in the sense that, as the slope of the front diminishes with time, the singularities that we disregarded at $\Lambda = 0$ and $\Lambda = 1$ lose more and more of their

Results and Discussion

To evaluate and apply the theory, we need a value of the hydraulic conductivity of the coarse sand. Consequently, we fit the average measured slope of the front as a function of one over the square root of time by a least square error procedure (Figure 4). The slope of the fitted line permits determination of the hydraulic conductivity value used for theoretical purposes. The value for the intercept approaches 0, which, together with $R^2 \rightarrow 1$, shows the validity of the theory presented and of the method used for the hydraulic conductivity determination. The average hydraulic conductivity of the coarse sand was found to be 3.2 cm/min, a value that is 1.5 times less than an independent determination by the constant head method applied to a 50 cm long sand column. Figure 5 shows a comparison between the fronts obtained with a normalized form of Equation 14 and those obtained experimentally. In general, agreement exists between the theoretical and experimental locations of the front, even though the presence of the inflow chamber, containing

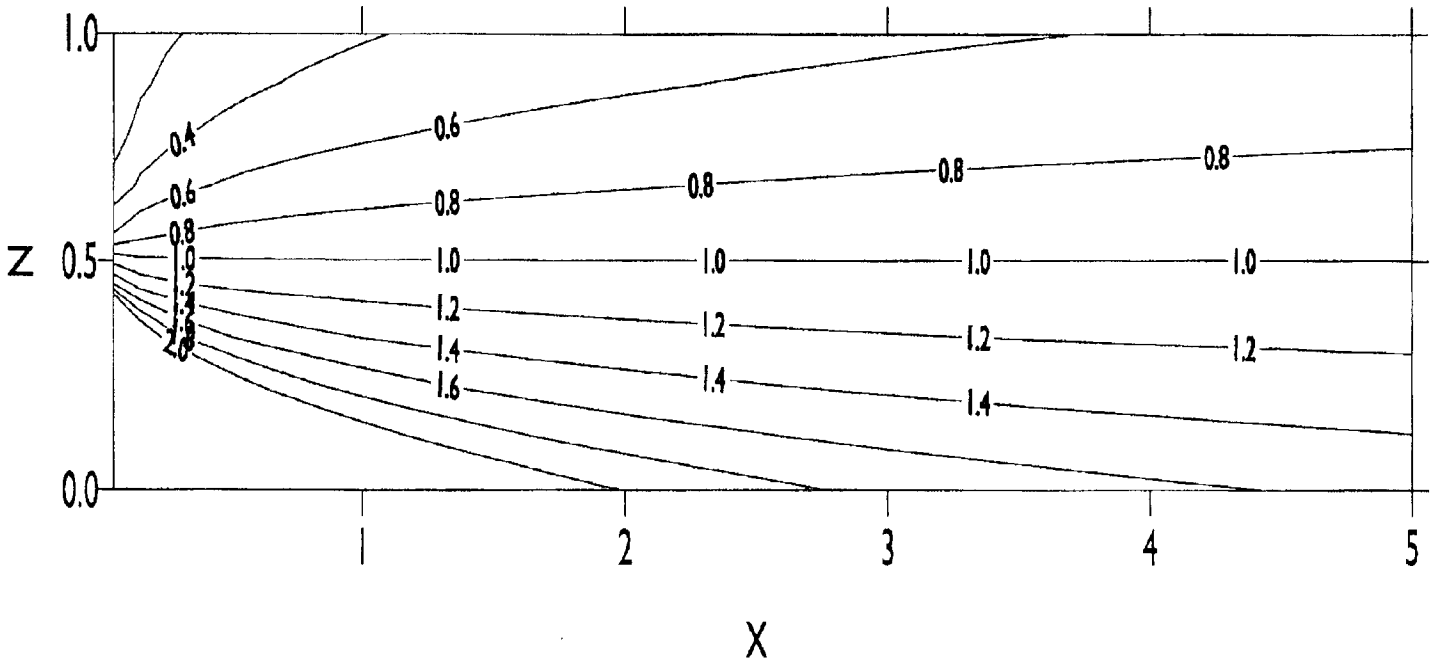

Figure 7. Nondimensional apparent velocity, Ω, as a function of the nondimensional variables (X,Z).

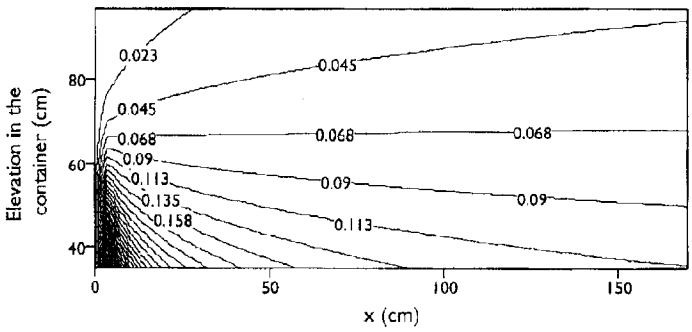

Figure 8. Normalized apparent velocity, ω, for the intermediate-scale flow container.

importance. The occurrence of relatively small lenses, with saturated hydraulic conductivity values less than the remainder of the porous medium, demonstrate that the presence of small scale heterogeneities has little influence on the overall flow behavior, which compares favorably to the solution described by Equation 14. We observed that, even if the flow through a lens was limited, the density difference caused the salt water present above the lens to come down when it reached the end of the lens. It then formed a uniform salt front again with the salt water that flowed under the lens (Figure 6). The general trend for the moving front is thus to alleviate the influence of heterogeneities and to behave according to Equation 14, as if the porous medium is homogeneous. A comparison with the situation that would occur in case no density difference exists between the tracer solution and the ambient water (Figure 6) shows that values of the apparent dispersivity due to heterogeneity, obtained with dense tracers, will be lower than those obtained with tracers having the same density as water because of a higher vertical mixing.

A contour plot of the nondimensional apparent velocity field Ω (Equation 16) is presented in Figure 7, while the normalized theoretical apparent velocity field, Ω, is given in Figure 8. The compared values of apparent velocities (Figure 9), obtained by the theoretical approach (italic) and by fitting with CXTFIT2 (roman), are generally in agreement.

Applications

Hydraulic Conductivity Values

In many instances, both in laboratory flow containers and in the field, conservative tracers are used to determine the horizontal saturated hydraulic conductivity of a porous medium (e.g., Molz et al. 1990). To obtain the necessary flow velocity in a presumably homogeneous porous medium, the program CXTFIT2, or some other one-dimensional fitting program, is used to analyze the breakthrough curves obtained in response to a step input. Not taking density differences between the tracer solution and the ambient water into account may, however, lead to a considerable error. Considering the problem strictly one-dimensional, there usually is no concern about the depth of sampling and only the longitudinal distance between the injection and extraction point is thought to be important. Based on the theory we provided, we will derive an expression for the relative uncertainty due to density effects on the obtained K value. From the Darcy equation, we know that for a given hydraulic gradient (ΔH/ΔL), K is proportional to the velocity of the displacement of the front in one dimension. The relative uncertainty can thus be defined as the difference between the maximum, Ω_{max}, and the minimum nondimensional apparent velocity, Ω_{min}. These extreme values are obtained for Z = 0 and Z = 1, respectively, which according to Equation 16 results in

$$\Omega_{max} = \frac{X}{\left(\frac{1}{2} - \frac{1}{2}\sqrt{1 + 4X}\right)^2} \qquad (18a)$$

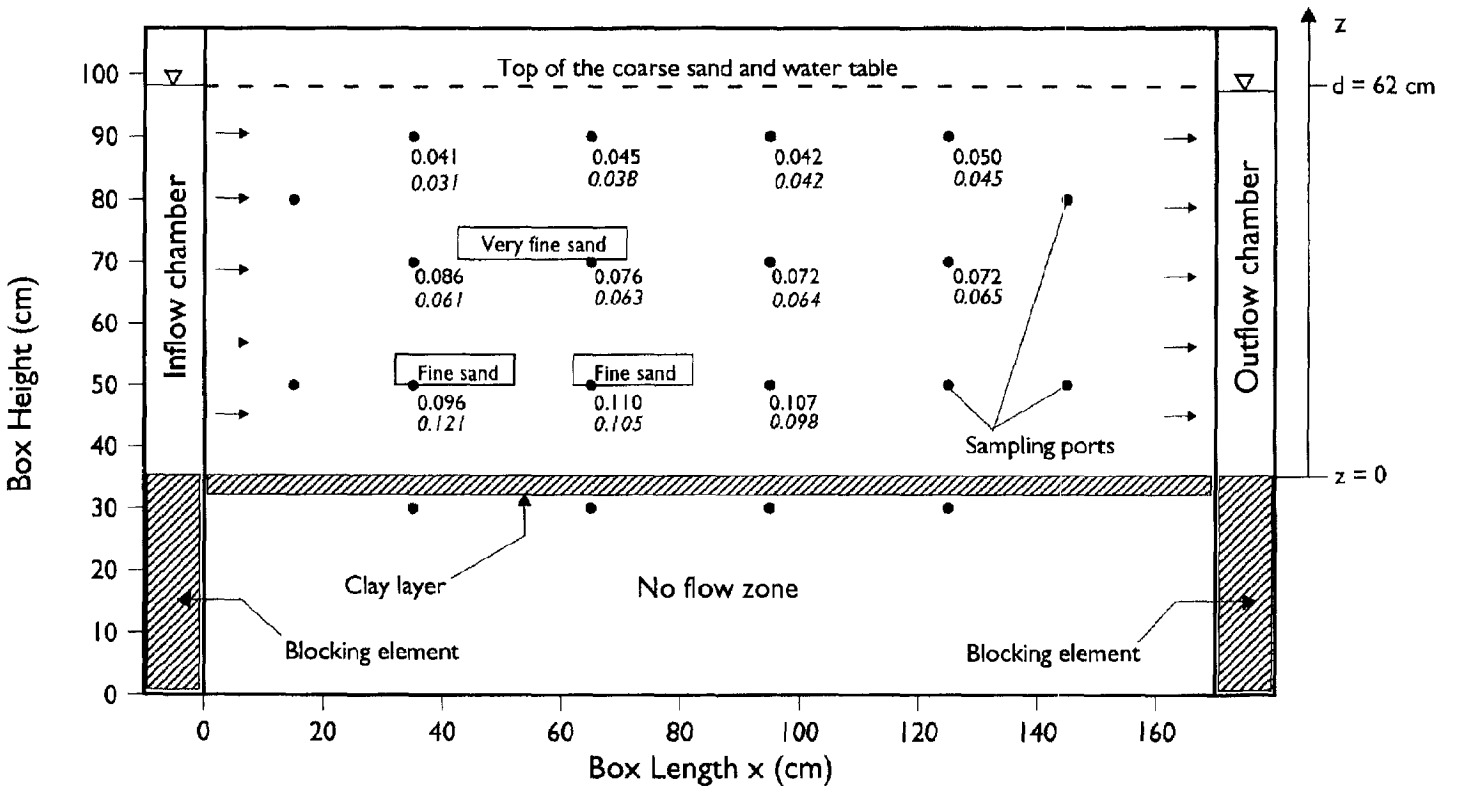

Figure 9. Sketch of the intermediate-scale flow container and comparison between velocity values obtained by breakthrough curve fitting at sampling ports (roman values) and by application of Figure 8 (italic values).

$$\Omega_{min} = \frac{X}{\left(-\frac{1}{2} - \frac{1}{2}\sqrt{1 + 4X}\right)^2} \tag{18b}$$

The relative error in K can be expressed as

$$\frac{\Delta K}{K} = |\Omega_{max} - \Omega_{min}| = \frac{16X\sqrt{1 + 4X}}{(-1 + \sqrt{1 + 4X})^2 (1 + \sqrt{1 + 4X})^2} \tag{19}$$

For X » 0.25, the preceding equation becomes

$$\frac{\Delta K}{K} \approx \frac{2}{\sqrt{X}} \tag{20}$$

Figure 10 compares the plots of Equation 19 (solid line) and Equation 20 (dashed line). For all practical purposes, X > 1 is a sufficient condition for the use of Equation 20 instead of Equation 19.

After normalization, Equation 20 can be written as

$$\frac{\Delta K}{K} \approx 2\sqrt{\frac{\left(\frac{\Delta\gamma}{\gamma}\right)\cdot d}{\left(\frac{\Delta H}{\Delta L}\right)\cdot x}} \tag{21}$$

As an example, consider the case of using a conservative tracer such that the relative density difference is 1%. Furthermore, assume a hydraulic gradient of 1% (1 cm/m) and a tracer travel distance of four times the depth of the aquifer. This results in a relative uncertainty value for the hydraulic conductivity of about 100%.

Dispersivity Values

For determining the dispersivity of a porous medium conceptualized as homogeneous in which flow occurs in the horizontal direction, breakthrough curves can be obtained, for example, at a downstream fully penetrating end chamber, in response to a step input. We will further assume the use of a conservative tracer, the solution of which is denser than the water it will displace. Ignoring the density difference in the analysis by a one-dimensional program such as CXTFIT2, the value of the apparent dispersion coefficient comes into question because the shape of the breakthrough curve is to a large extent determined by the gradual arrival of the gravity-induced sloped front and little by dispersion effects.

For comparison of the density-induced spreading with a purely advective-dispersive process, we consider the BVP consisting of the one-dimensional advection-dispersion equation

$$\frac{\partial c}{\partial t} = D\frac{\partial^2 c}{\partial x^2} - V\frac{\partial c}{\partial x} \tag{22}$$

subjected to the boundary conditions analogous to Equation 2:

$$c(x,0) = c_0 \qquad \text{for } x < 0 \tag{23a}$$

$$c(x,0) = 0 \qquad \text{for } x > 0 \tag{23b}$$

$$c(-\infty,t) = c_0 \tag{23c}$$

where V (LT^{-1}) is the pore water velocity, D (L^2T^{-1}) is the dispersion coefficient, c (ML^{-3}) is the concentration of the tracer, and c_0 is the inlet concentration. The solution to this BVP was given by von Rosenberg (1956) and restated in Bear (1972):

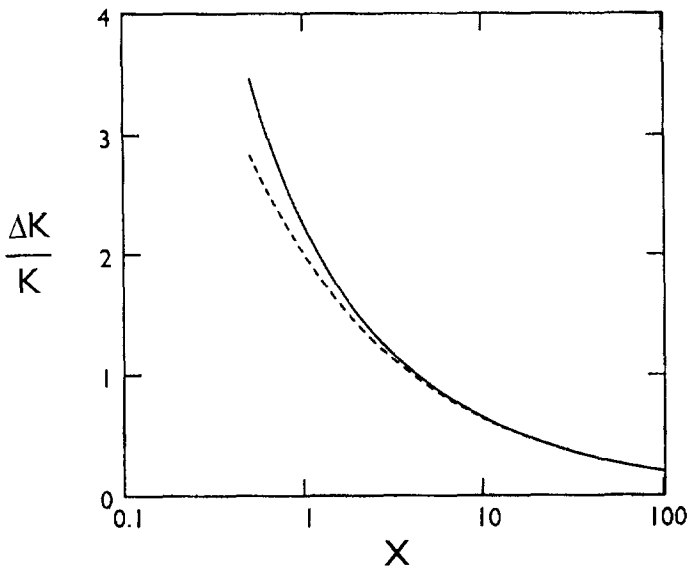

Figure 10. Uncertainty due to density-difference effects in the hydraulic conductivity determination, in case of a rectangular porous medium subjected to a conservative tracer at a step input. The solid line represents Equation 19 and the dashed line the approximate solution Equation 20.

$$\frac{c}{c_0} = \frac{1}{2}\left[1 \pm \operatorname{erf}\frac{x - Vt}{2\sqrt{Dt}}\right] \quad \begin{matrix} + \text{ for } x - Vt < 0 \\ - \text{ for } x - Vt > 0 \end{matrix} \tag{24}$$

It is important to note the analogy between the forms of Equations 14b and 24, which shows that the gradual arrival of solute due to the sloped front (Equation 14) can be conceptually compared with a dispersion process (Equation 24). Applying the concept of mixing length L_m (Taylor 1953), which is defined as the distance between the locations where $c/c_0 = 0.1$ and $c/c_0 = 0.9$, to Equation 24 results in

$$D = \frac{1}{t}\left(\frac{L_m}{3.625}\right)^2 \tag{25}$$

In case of the approximate solution, i.e., a sloped, linear front between the tracer solution and fresh water, L_m becomes according to Equation 13

$$L_m = 1.6\sqrt{\frac{dK't}{n}} \tag{26}$$

Substitution of Equation 26 into Equation 25 gives an estimate of the apparent dispersion coefficient associated with the gradual arrival of the tracer under the influence of gravity effects only:

$$\widetilde{D} \approx 0.2\frac{d \cdot K}{n}\left(\frac{\Delta\gamma}{\gamma}\right) \tag{27}$$

This result differs by a factor of 5 from the dispersion coefficient used by Gelhar et al. (1972) in their study of axisymmetric gravitational mixing. In case of the intermediate-scale experiment used for validation of Equation 14, we obtained a $\widetilde{D}$ value of about 1.5×10^{-2} cm^{2}s^{-1}. For comparison, values obtained by fitting CXTFIT2 through the breakthrough curves obtained from sampling ports (point measurements), values that are mainly due to dispersion processes, were in the order of 1.5×10^{-4} cm^{2}s^{-1}. The difference of two orders of magnitude shows the necessity of taking gravity effects into account when using a dense conservative tracer arriving in an end chamber or a well perforated over its total height. In case of a heterogeneous porous medium, we already noticed (Results and Discussion) that the use of a dense tracer, by increasing vertical mixing, has the tendency to reduce the influence of heterogeneity on flow. On the other hand, a density difference induces a gradual arrival of the tracer (Equation 27). These two influences have opposite effects on the dispersivity value obtained in a dense tracer experiment. Nevertheless, it would be a mistake to neglect these effects, for one influence does not a priori eliminate the other one.

We would like to emphasize that $\widetilde{D}$, as expressed in Equation 27, is independent of the flow velocity, which is inconsistent with the notion of diffusion/dispersion in porous media. $\widetilde{D}$ is also independent of x. The presence of a sloped front due to specific gravity differences between the tracer solution and the ambient water has, therefore, no influence on the dependency of the dispersivity on the longitudinal distance, as reported at the field scale (Gelhar 1993). However, as dense tracers are being widely used, ignoring density-difference effects may be the cause of many erroneous dispersivity values, as dispersivity is supposed to be a measure of the structure and/or heterogeneity of the porous medium only.

These two applications show the importance of density-difference effects on results obtained with tracers. The nondimensional solution described by Equation 14 is nevertheless restricted to the case of a two-dimensional rectangular homogeneous porous medium, which is restrictive compared with the complexity present in field experiments. The incorporation into further research of concepts such as well solutions, heterogeneity, slug size, instabilities (e.g., Oostrom et al. 1992; Liu and Dane 1996), will be necessary to reach a more complete understanding of the influence of density differences on tracer experiments.

Conclusion

We developed an approximate solution to the problem of a sharp salt water/fresh water moving interface, which by its nondimensional nature is easily applicable to every case of a rectangular homogeneous porous medium. The agreement with experimental data tends to show a weak influence of the boundary conditions on the general trend of the density affected flow. The solution allows for a simplified general view of the influence of density differences upon values of velocity, permeability, or dispersivity obtained in conservative tracer experiments.

Acknowledgments

This research was carried out as part of the U.S. Environmental Protection Agency project R825409 "Investigation of the entrapment and surfactant enhanced recovery of nonaqueous phase liquids in heterogeneous sandy media."

We would like to thank Laurent Bahaminyakamwe (Auburn University) and Cor Hofstee (Universität Stuttgart) for their contributions to the experiments.

The reviewers (Drs. Raffensperger, Spiegel, and Halford) are acknowledged for their suggestions, which culminated in an improved manuscript.

References

Bear, J. 1972. *Dynamics of Fluids in Porous Media.* New York: Elsevier.

Bear, J., and G. Dagan. 1964. Moving interface in coastal aquifers. In *Proc. Amer. Soc. Civil Eng. Hydraul. Div.* No. 4, 90: 193-215.

Gelhar, L.W. 1993. *Stochastic Subsurface Hydrology.* Englewood Cliffs, New Jersey: Prentice Hall.

Gelhar, L.W., J.L. Wilson, and J.S. Miller. 1972. Gravitational and dispersive mixing in aquifers. In *Proc. Amer. Soc. Civil Eng. Hydraul. Div.* No. 12, 98, 2135-53.

Liu, H.H., and J.H. Dane. 1996. A criterion for gravitational instability in miscible dense plumes. *Journal of Contaminant Hydrology* 23, 233-243.

Molz, F.J., O. Güven, J.G. Melville, and C. Cardone. 1990. Hydraulic conductivity measurements at different scales and contaminant transport modeling. In *Dynamics of Fluids in Hierarchical Porous Media,* ed. J.H. Cushman. New York: Academic Press.

Oostrom, M., J.S. Hayworth, J.H. Dane, and O. Güven. 1992. Behavior of dense aqueous phase leachate plumes in homogeneous porous media. *Water Resources Research* 28, no. 8: 2123-2134.

Oostrom, M., C. Hofstee, R.C. Walker, and J.H. Dane. 1999. Movement and remediation of trichloroethylene in a saturated heterogeneous porous medium. *Journal of Contaminant Hydrology* 37, 159-178.

Taylor, G.I. 1953. Dispersion of soluble matter in solvent flowing slowly through a tube. In *Proc. Roy. Soc. A,* No. 1137, 219, 186-203.

Toride, N., F.J. Leij, and M.Th. van Genuchten. 1995. The CXTFIT code for estimating transport parameters from laboratory or field tracer experiments. U.S. Salinity Laboratory Research Report No. 137, U.S.D.A., Riverside, California.

von Rosenberg, D.U. 1956. Mechanics of steady state single phase fluid displacement from porous media. *J. Amer. Inst. Chem. Eng.* 2, 55-58.